

# Growth, structure, and magnetic properties of thin Mn films epitaxially grown on (001) bcc Fe

S. Andrieu

*LPM, CNRS/Université Nancy, 54506 Vandoeuvre, France*

M. Finazzi\*

*LURE CNRS/CEA/Université Paris-sud, 91405 Orsay, France*

Ph. Bauer and H. Fischer

*LPM, CNRS/Université Nancy, 54506 Vandoeuvre, France*

P. Lefevre and A. Traverse

*LURE CNRS/CEA/Université Paris-sud, 91405 Orsay, France*

K. Hricovini

*LPMS, Université Cergy-Pontoise, 95011, Cergy-Pontoise, France*

G. Krill

*LURE CNRS/CEA/Université Paris-sud, 91405 Orsay, France*

M. Piecuch

*LPM, CNRS/Université Nancy, 54506 Vandoeuvre, France*

(Received 8 July 1997)

This work is dedicated to the study of structural and magnetic properties of Mn films epitaxially grown on (001) bcc Fe. At room temperature, the Mn growth mode on (001) Fe is observed to be layer by layer, without any interdiffusion, as shown by reflection high-energy electron-diffraction and Auger spectroscopy. Moreover, Mn is observed to segregate on top of the Fe surface. Two-dimensional pure Mn films are thus grown and the structural and magnetic properties of these Mn films are investigated by *in situ* and *ex situ* x-ray absorption (EXAFS) and magnetic circular dichroism. For uncapped Mn films, a structural and magnetic transition is observed between 2 and 3 Mn monolayers. Up to 2 Mn atomic planes, the EXAFS oscillations are consistent with calculated EXAFS spectra assuming a bct structure close to the Fe bcc structure. A ferromagnetic behavior is observed in these films. From 3 to 10 atomic planes, the Mn film structure changes and the ferromagnetic behavior disappears. Moreover, EXAFS analysis shows that this structural transition occurs at higher thicknesses for Fe capped Mn films. Nevertheless, the ferromagnetic behavior observed on 0–2-ML-thick uncapped Mn films is no more stable in thick bct Mn films capped by Fe. [S0163-1829(98)03303-7]

## I. INTRODUCTION

For about 20 years, a large amount of theoretical work has been dedicated to the interrelation between structure and magnetic properties of transition metals. The comparison between theoretical predictions and experimental investigations was limited however, because of the technical difficulties to prepare sufficiently strained materials (high pressures and/or high temperatures). This limitation was bypassed by growing strained or metastable metallic films using molecular-beam epitaxy (MBE).<sup>1</sup> Indeed, in the last decade, metallic films with strained or unusual crystalline structures (i.e., not stable in the regular conditions of pressure and temperature) were epitaxially grown on appropriate substrates or buffer layers in order to investigate their magnetic properties. The best illustrating example is undoubtedly fcc Fe/(001) Cu system, which has been one of the most extensively studied systems.<sup>2</sup>

One of the general trends predicted by the theoretical studies is the increase of the magnetic moment when the atomic volume is increased.<sup>3</sup> The magnetic moment of the

free atom is reached for a large atomic volume. According to Hund's rule, Mn is thus an interesting candidate to be studied since the magnetic moment of the free Mn atom is as large as  $5\mu_B$  (half-filled  $d$  shell). However, in bulk metallic structures like Mn $\alpha$ , Mn $\beta$ , and fcc Mn (characterized by a small atomic volume  $\approx 12 \text{ \AA}^3/\text{atom}$ ), Mn is always found to be in an antiferromagnetic (AF) state.<sup>4</sup> For these reasons, a number of experimental works have been performed in order to grow Mn in crystalline structures with larger atomic volumes. However, a large atomic volume is not a sufficient condition to observe a high spin ferromagnetic state. Indeed, an AF state is shown to be the lowest energy configuration for fcc Mn, even for large volumes.<sup>5</sup> In the case of nonuniformly strained fcc Mn structures (fct), no theoretical predictions were available for a large range of the  $c/a$  ratio. Up to now, all the strained Mn structures prepared on Ru, Ni,<sup>6</sup> Al,<sup>7</sup> Pd,<sup>8</sup> Cu, Ag,<sup>9</sup> Co,<sup>10</sup> and Ir (Ref. 11) buffer layers are shown to derive from a distortion of the fcc Mn structure. A volume increase up to 10% is reached but an AF (or nonmagnetic) behavior was always observed. These experimental results

show that these distortions (trigonalization or tetragonalization) of the fcc Mn structure are not sufficient to obtain Mn in a ferromagnetic state.

At variance with the fcc Mn structure, a ferromagnetic behavior is predicted for bcc Mn.<sup>12</sup> However, to our knowledge, nobody managed to grow Mn in a—even strained—bcc structure in thin films. Finally, several recent theoretical studies have shown that the magnetic properties of ultrathin films can be much different from the ones in the bulk. However, the magnetic properties of 1- or 2-ML-thick magnetic films are difficult to study using macroscopic techniques. Recently, x-ray magnetic circular dichroism has been shown to be a powerful tool to measure the magnetic contribution of very small amounts of materials. O'Brien and Tonner<sup>13</sup> actually observe a ferromagnetic ordering of ultrathin Mn films (i.e., in the monolayer range). These promising results, added to the fact that bcc Fe is a good candidate to grow Mn in a bcc structure, motivated us to investigate the magnetic properties of Mn films epitaxially grown on a (001) bcc Fe surface.

We have actually observed a Mn ferromagnetic behavior in ultrathin Mn films grown on (001) Fe in the thickness range between 0 and 2 ML thick.<sup>14</sup> Rather small magnetic moments compared to theoretical predictions are observed and the alignment between interfacial Mn and Fe moments is found to be parallel.<sup>14,15</sup> However, a number of questions still remain to be addressed. First of all, several recent calculations are devoted to the Mn/(001) Fe system, leading to different lowest-energy spin configurations.<sup>16</sup> All these theoretical studies are performed assuming an in-plane parameter equal to the Fe one, and an out-of-plane parameter equal to 3.27 Å, as reported in Ref. 17. However, this value has to be confirmed for ultrathin Mn films. *In situ* x-ray absorption spectroscopy (EXAFS) and reflection high-energy diffraction (RHEED) experiments are performed in order to characterize quantitatively the structure of Mn films grown on (001) Fe. Moreover, we show in this study that the Mn ferromagnetic behavior is observed to disappear above 2 ML. EXAFS and RHEED experiments are also performed to investigate the possible intervention of a structural modification accompanying this magnetic transition. Finally, the structural and magnetic properties of Mn/Fe(001) superlattices are studied in order to test the influence of the Fe capping. In the first part of this paper, details about the experimental setup are presented. The second part is dedicated to the study of the characteristics of the Mn layers, i.e., (i) growth (growth mode, relaxation, interdiffusion, segregation), (ii) structure, and (iii) Mn magnetic properties. The results are discussed and summarized in the last part.

## II. EXPERIMENTAL DESCRIPTION

Auger electron spectroscopy (AES) was used to study (i) the chemical quality of the Fe and Mn surfaces, (ii) the Mn interdiffusion in Fe, and (iii) the Mn segregation on top of growing Fe films. As the Mn and O contributions are mixed in AES but not in x-ray photoelectron spectroscopy (XPS), XPS was also performed on Mn films. The surface lattices, growth mode, and in-plane parameter variation during the Mn growth were studied by RHEED. The three-dimensional structure of the Mn films uncapped by Fe were studied *in situ*

by EXAFS. The structures of Mn and Fe in Mn/Fe superlattices were also studied by *ex situ* EXAFS experiments. These experiments were performed on the DCI ring at LURE. The Mn magnetic properties were determined by x-ray magnetic circular dichroism (XMCD) experiments performed at the Super-Aco ring at LURE. All the *in situ* experiments (growth, structural, and magnetic analyses) were performed in UHV with a base pressure of less than  $10^{-10}$  torr. The samples have been prepared and analyzed in three MBE systems: our own MBE in Nancy, the MBE coupled to the XMCD chamber at LURE, and the EXAFS MBE chamber at LURE. In the XMCD and home MBE, the chemical quality is checked by AES and XPS and the growth is controlled by RHEED. In *in situ* EXAFS experiments, AES and LEED facilities are available.

In each chamber, Fe and Mn are sublimated by using Knudsen cells, with typical growth rates from 1 to 4 Å/min, calibrated using RHEED oscillations and/or quartz microbalance located at the place of the sample. The Mn layers are grown at room temperature (RT) on thick Fe buffer layers (200–500 Å). No oxygen and carbon contamination is observed on either Mn and Fe surface obtained at room temperature. The Fe buffer layers are grown at RT on (001) MgO substrates and annealed at around 750 K in order to obtain flat surfaces with large terraces. However, if no carbon contamination is observed on Fe surfaces annealed up to 650 K, a small carbon contamination is always observed on the surface of Fe buffer layers annealed up to 750 K. The dichroic experiments were performed on both C contaminated (annealing up to 750 K) and uncontaminated (annealing below 650 K) Fe surfaces. We have not observed any influence of this small C contamination on our results.

The EXAFS experiments were performed at the Mn *K* edge with in- and out-of-plane polarizations. After background removal, the EXAFS oscillations are extracted and normalized to the height of the absorption step edge. As the resulting oscillations are characteristic of the chemical and structural environment of the absorbing atom, the Mn structure can be determined by simulating these oscillations. The theoretical EXAFS oscillations are calculated using the multiple-scattering approach (FEFF code 6, Ref. 18). Using such analysis, we have actually shown that the simulated EXAFS oscillations obtained for Mn $\alpha$ , Mn $\beta$ , fcc, bcc, and three-dimensional Cu<sub>2</sub>Mg or Zn<sub>2</sub>Mg Laves phase are much different from one another.<sup>11</sup> The three-dimensional (3D) structure of a Mn film can thus be confirmed comparing the experimental and simulated EXAFS oscillations.<sup>11</sup>

The XMCD measurements are performed with the magnetic field aligned with the photon beam, and with an angle of 20° between the direction of propagation of the photons and the sample surface. The Fe layers are magnetized along the (100) easy axis of magnetization of bulk Fe. The XMCD spectra are collected at room temperature by switching the direction of the magnetic field and measuring the total electron yield for each photon energy. The degree of polarization is equal to 70%, and the applied magnetic field is 250 Oe at the place of the sample. The dichroism signals are calculated by subtracting the absorption spectra obtained with positive and negative magnetic fields. The resulting dichroic signal is normalized to the intensity at the Mn *L*<sub>III</sub> edge calculated after background removal (same method as in Ref. 19), and

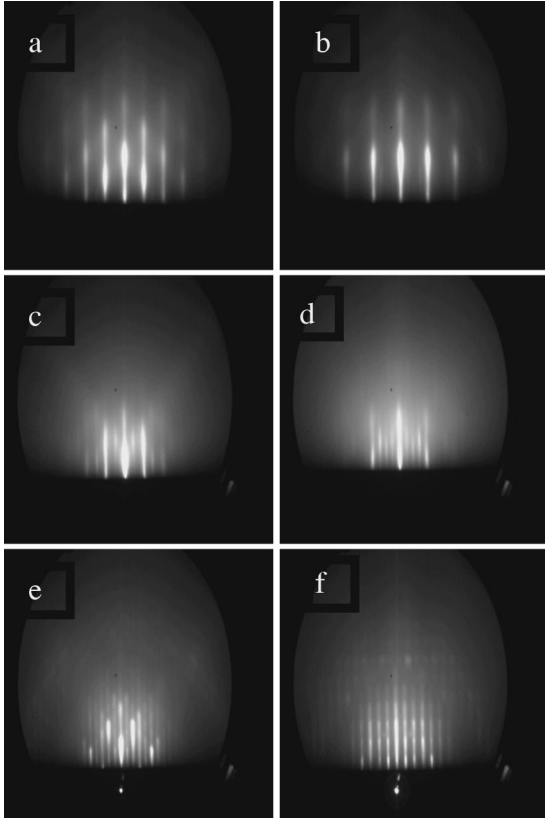


FIG. 1. RHEED pattern along (100) (a), (c), (e) and (110) (b), (d), (f) azimuth observed during the Mn growth at RT on (001) Fe up to 10 ML (a),(b), between 10 and around 17 ML (c),(d), and above 17 ML (e),(f).

corrected for the incomplete polarization and nonparallel alignment of magnetization and photon spin.

### III. EXPERIMENTAL RESULTS

#### Growth

Up to around 10 ML the in-plane structure of the Mn films was observed by RHEED to be identical to the (001) Fe plane (Fig. 1). Above this thickness, a  $C(4 \times 4)$  [or  $(2\sqrt{2} \times 2\sqrt{2})(R)45^\circ$ ] superstructure takes place. Finally, for large thicknesses, the RHEED patterns again change (Fig. 1). These patterns are the same as the patterns observed on  $Mn\alpha$  thick films deposited on (001) Ir lattice. Thick Mn films deposited on (001) Fe thus relax in the  $Mn\alpha$  structure.

We have checked by Auger spectroscopy that Mn does not interdiffuse in Fe up to a substrate temperature around 450 K, as was previously shown by Walker and Hopster.<sup>20</sup> On the contrary, Mn is found to segregate on the surface of Fe capped samples during the Fe growth. This segregation phenomenon can be easily observed by AES and RHEED analysis. For this purpose, AES and RHEED experiments are performed on 0–30 ML-thick Fe films grown at room temperature on a 15 ML-thick Mn film. Note that a  $C(4 \times 4)$  surface structure is thus observed by RHEED for such thick Mn film. First of all, although the Fe growth mode is observed by RHEED to be layer by layer on Mn, *the Mn  $C(4 \times 4)$  surface structure is still observed even when the Mn layer is capped by up to 12 ML of Fe.* This segregation

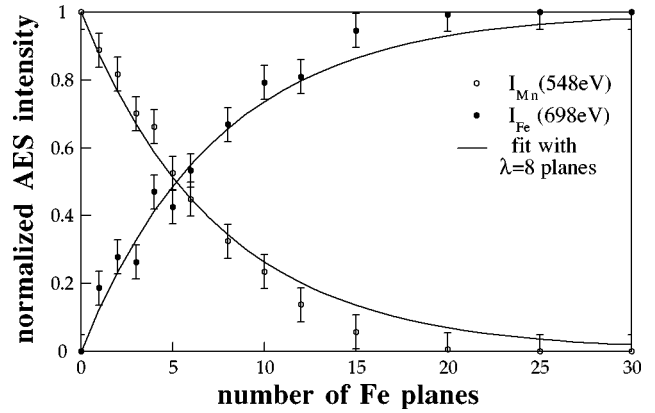


FIG. 2. Mn (548 eV) and Fe (698 eV) AES peaks intensity evolution with the number of deposited Fe atomic planes on top of 15-ML-thick Mn film (see text).

process is also evidenced by plotting the variation of the Mn (548 eV) and Fe (698 eV) AES peaks with the thickness of the top Fe film (Fig. 2). These AES curves are fitted with exponential laws:

$$I_{Mn} = I_{Mn}^{\infty} \exp(-n/\lambda \cos \theta),$$

$$I_{Fe} = I_{Fe}^{\infty} [1 - \exp(-n/\lambda \cos \theta)],$$

where  $\lambda$  is the mean free path of the electrons in the Fe film and  $\theta$  the angle between the sample normal and the detector ( $\theta = 20^\circ$  in our system). If Mn do not segregate on top of the growing Fe surface,  $\lambda$  should be equal to the Fe bulk mean-free path. We have measured this parameter on other systems [Fe/V(001), Fe/Ir(001)] and found  $\lambda = 5.4$  atomic planes. The fit reported in Fig. 2 is performed with  $\lambda = 8$  atomic planes. This large mean-free-path value added to the persistence of the  $C(4 \times 4)$  Mn superstructure up to 12 ML Fe confirms the Mn segregation on top of Fe. Note that in MBE such a segregation phenomenon can be explained by surface diffusion<sup>21</sup> (i.e., bulk diffusion is not necessary).

About ten RHEED oscillations are observed during the Mn growth on Fe (Fig. 3). The growth mode is thus layer by layer up to around 10 ML. However, after completing the

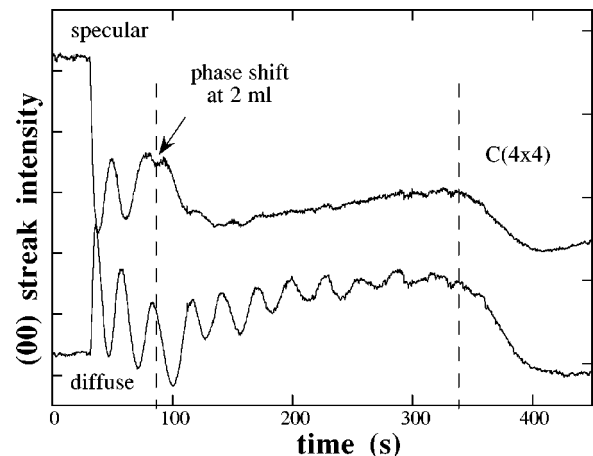


FIG. 3. RHEED oscillations observed at RT along (110) azimuth during Mn growth on Fe in specular (top) and grazing geometry (bottom).

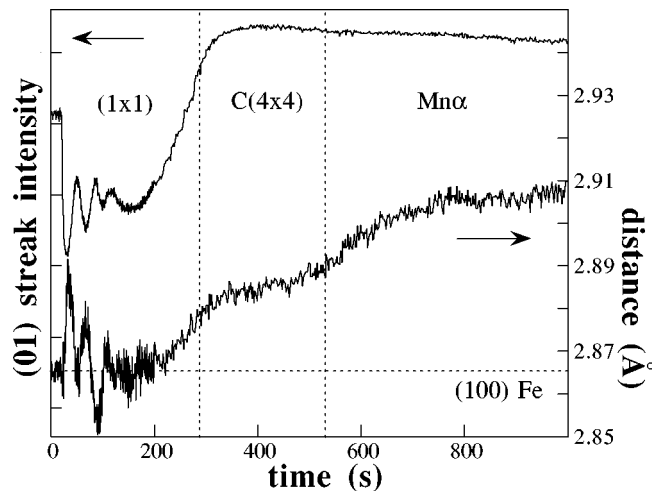


FIG. 4. (01) streak intensity and in-plane parameter temporal evolution during Mn growth on Fe at RT.

first 2 ML, an anomalous behavior is observed on RHEED oscillations obtained in specular geometry. This behavior is consistent with a structural modification (out-of-plane distance variation or pattern change). In grazing incidence geometry, this effect is, however, less observable (even if a larger period can be observed on the third oscillation). This is not surprising since the temporal evolution of the RHEED intensity is essentially due to a diffraction process in specular geometry and to diffusion of  $e^-$  waves by the step edges in grazing incidence geometry. Finally, the RHEED intensities stop to oscillate when the  $C(4 \times 4)$  superstructure takes place.

Information about structural changes can also be obtained by measuring the in-plane parameter variations during the Mn growth.<sup>22</sup> Such an experiment is reported in Fig. 4. Three regimes are observed. They are related to the three RHEED pattern sequences shown in Fig. 1. In this study, we are, however, only interested in the first regime, in which the Mn surface lattice is pseudomorphic to the Fe one. In this regime, two main features are observed in Fig. 4. First, at the beginning of growth, the in-plane parameter is observed to oscillate in antiphase with the intensity oscillations registered in specular geometry. This effect is explained in terms of elastic relaxation as proposed in Ref. 22. In our opinion, this oscillatory behavior is rather due to surface stress relaxation. It should be noted that such a result is only obtained on high chemical and structural quality Fe surfaces (large terraces). This result demonstrates that the Mn layers are compressed and pseudomorphic to the Fe lattice at least up to 2 ML. The second point is that above 2 ML, the surface stress is relaxed (the in-plane parameter oscillatory behavior disappears) and the in-plane parameter smoothly varies. This is another confirmation of a structural change.

Obviously, the three-dimensional structure of these Mn film cannot be determined by using RHEED. However, details on the 3D structure can be specified. First of all, the  $1 \times 1$  surface lattice is still observed above 2 ML up to 10 ML. This means that the surface lattice has not changed during the structural relaxation. Moreover, the time needed to complete a monolayer does not change below 2 ML and above 3 ML. This means that the cell pattern is always 1 Mn atom per lattice site. This structural modification can thus

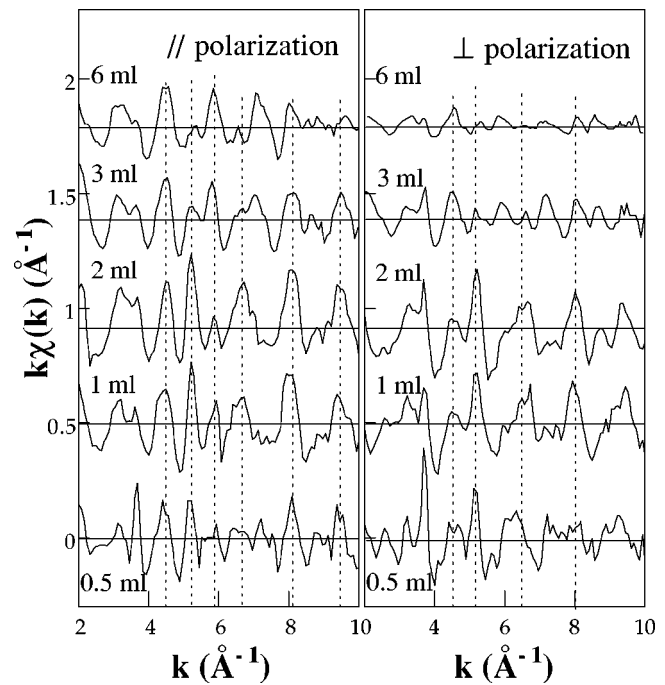


FIG. 5. *In situ* EXAFS spectra measured at 77 K on 0.5–6 ML-thick Mn films. Note the oscillations drastic change between 2 and 3 ML. The dashed lines are just here to guide the eyes.

only be explained by a variation of the crystallographic parameters or/and a change of nucleation site.

### Structural properties

The *in situ* EXAFS experiments were performed on 0.5-, 1-, 2-, 3-, and 6-ML-thick Mn films deposited on Fe (Fig. 5). One can easily see that the EXAFS oscillations clearly change between 2 and 3 ML, which confirms the structural transition.

The AES analysis allows us to verify that such structural transition does not come from any interdiffusion or oxidation of the Mn films. This is moreover confirmed by EXAFS analysis. In order to test a possible interdiffusion process, a 6-ML-thick Mn film was intentionally annealed at 650 K. Mn/Fe interdiffusion is actually observed by AES in this case. The EXAFS oscillations (Fig. 6) are then totally different from the EXAFS spectra measured on unannealed films (Fig. 5). Any oxidation process is also eliminated since the

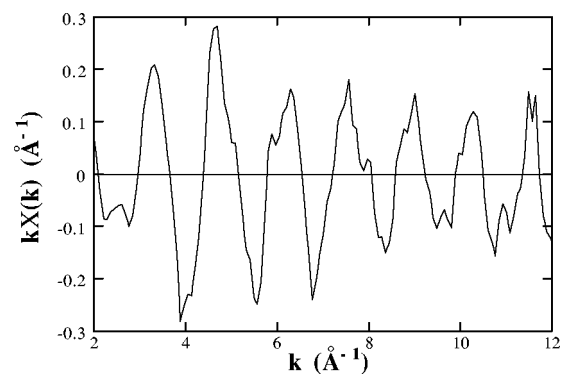


FIG. 6. Experimental EXAFS oscillations observed for both polarizations on a 6 Mn ML film interdiffused with Fe at 650 K.

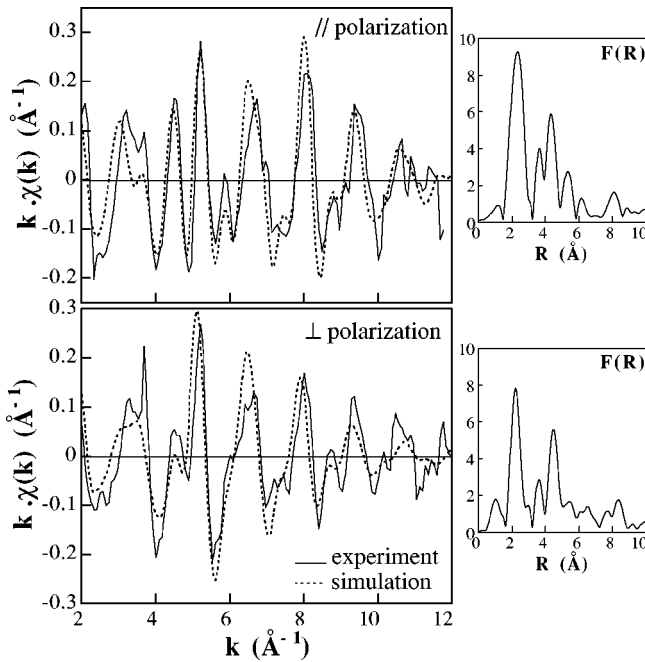


FIG. 7. Left: experimental and calculated EXAFS oscillations for 2 Mn ML/(001) Fe (see text). Right: Fourier transforms which show the distinctive double-peak bcc structure.

EXAFS spectra calculated for the seventh tabulated manganese oxide structures are much different from the observed EXAFS spectra. These points being confirmed, we now try to determine the Mn structures in these films.

In the case of ultrathin films, the EXAFS oscillations cannot be compared to the simulations calculated assuming a “bulk” structure. Indeed, the number of neighbors is limited in the growth direction. Moreover, the chemical environment and the distances between (001) planes are not necessarily the same from the interface to the surface of the Mn film. This fact leads to several inequivalent absorbing atoms. For a 1-ML-thick Mn film, there is only one kind of absorbing atom. But for a 2-ML-thick Mn film, there are two different Mn absorbing atoms (at the Mn/Fe interface, and in the Mn surface). Finally, for the same reason, three different absorbing Mn atoms must be taken into account for a 3-ML-thick Mn film. The EXAFS oscillations are calculated by adding the EXAFS amplitudes calculated for each absorbing atom.

A bct structure is used to simulate the EXAFS oscillations of the Mn films, in agreement with Ref. 17. Up to 2 Mn ML, the best fit is obtained using an in-plane parameter  $a_{\parallel}$  equal to the Fe one (2.87 Å) according to our RHEED results. The out-of-plane distance  $a_{\perp}$  between the Fe underlayer and the Mn monolayer is found equal to  $1.48 \pm 0.02$  Å. The distance between the first and second Mn layer is slightly increased ( $1.52 \pm 0.02$  Å). The comparison between experimental and calculated EXAFS spectra for a 2 Mn ML sample are shown in Fig. 7. The bct structure is thus confirmed up to 2 ML. The Debye temperatures for in-plane (250 K) and out-of-plane (200 K) polarizations are found to be smaller than the bulk one (410 K). This is not surprising since the Mn layers are almost two-dimensional. This bct structure is consequently close to the bcc Fe structure, as illustrated by the distinctive double peak observed on the Fourier transform (Fig. 7), typical of a bcc structure.

For thicker Mn layers, the EXAFS oscillations drastically change and obviously cannot be fitted by assuming this former bct structure. As the RHEED analysis allows us to assume that the structure is always bct with an in-plane parameter close to the Fe one, the simulations are performed for bct structures with  $a_{\parallel} = 2.87$  Å and different  $a_{\perp}$  values. The situation is, however, more involved than for 1- or 2-ML-thick Mn films. For the 3-ML-thick Mn films, three different out-of-plane distances should be taken into account, i.e., the distance between the first Mn layer and the underneath Fe layer,  $d_{\text{int}}$ , the distance between the first and the second Mn layer,  $d_{\text{mid}}$ , and the distance between the second and the surface Mn layer,  $d_{\text{surf}}$ . As a starting point we arbitrarily assume that  $d_{\text{mid}} = d_{\text{surf}}$ .

According to the results of Purcell *et al.*<sup>17</sup> and the results of Kim *et al.*<sup>24</sup> concerning thick Mn films, we have first simulated the EXAFS spectra of a bct structure with  $d_{\text{mid}} = 1.62$  Å and  $d_{\text{int}} = 1.47$  Å. The simulated EXAFS oscillations are found to be much different from the experimental ones observed above 2 ML. Keeping this  $d_{\text{mid}} = 1.62$  Å value, simulations were performed by varying  $d_{\text{int}}$  from 1.43 to 1.62 Å. Again, no agreement between experimental and simulated EXAFS is obtained. Finally,  $d_{\text{mid}}$  was varied from 1.6 to 1.9 Å. Good fits for in-plane polarization are obtained for  $d_{\text{mid}}$  in the range 1.7–1.8 Å. However, we do not manage to correctly fit the EXAFS oscillations for out-of-plane polarization. This means that the assumption  $d_{\text{mid}} = d_{\text{surf}}$  is not valid. Indeed, the intensity of the EXAFS oscillations for the out-of-plane polarization is very small, which can be explained by the occurrence of several different distances between Mn (001) planes when the Mn film thickness is increased.

To conclude, even if distance values between Mn (001) planes cannot be accurately determined, the modifications of the EXAFS spectra observed between 2 and 3 ML are due to an increase of the distance between Mn (001) planes.

*Ex situ* EXAFS experiments were also performed on Mn/Fe superlattices. The effect of Fe deposition on top of a bct Mn layer is thus investigated. Surprisingly, we find that the Mn EXAFS spectra observed on a  $(\text{Mn}_{6\text{ML}}\text{Fe}_{10\text{ML}}) \times 30$  superlattice (Fig. 8) are identical to those observed on the 2-ML-thick Mn film without any Fe capping. The only differences are first, a higher intensity of the EXAFS oscillations in the superlattice and second, a lower  $a_{\parallel}$  value. This is however not surprising since it simply means first, that the Debye temperature is increased in a superlattice compared to a thin Mn film and second, that Fe is also strained by Mn. The best fit is obtained for a bulk bct Mn structure with  $a_{\parallel} = 2.84 \pm 0.02$  Å and  $a_{\perp} = 3.00 \pm 0.04$  Å (Fig. 8). This Mn bct structure is thus stable up to at least 6 ML when Mn is capped by Fe. This higher critical thickness can be explained by the fact that Fe is also strained by Mn. It should be noted however, that a sufficient amount of Fe is necessary to avoid Mn relaxation during the superlattice growth. Indeed, Mn was found to relax when it is grown in a  $(\text{Mn}_{5\text{ML}}\text{Fe}_{5\text{ML}}) \times 50$  superlattice.

### Magnetic properties

XMCD experiments are performed *in situ* on Mn films in the thickness range from 0.3 to 10 ML thick. First of all, we

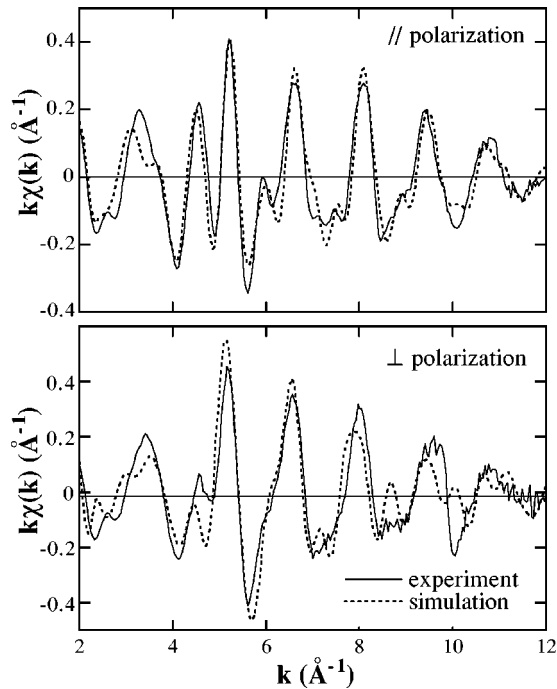


FIG. 8. Mn EXAFS spectra observed on a  $(\text{Mn}_{6\text{ML}}\text{Fe}_{10\text{ML}}) \times 30$  superlattice, and comparison with simulations (Mn bct,  $a_{\parallel} = 2.83 \text{ \AA}$ ,  $a_{\perp} = 3 \text{ \AA}$ ) for both polarizations.

must point out that a “metallic” shape, i.e., without fine structure, is always observed for the Mn- $L_{\text{II}}$ - $L_{\text{III}}$  absorption edge.<sup>14,15</sup> This result contrasts with the results reported in Ref. 23. This means that in our case, an atomic description for the Mn atoms is not correct, even for a 0.3-ML-thick film.

Up to 2 ML, a ferromagnetic behavior was observed on Mn, as reported in Ref. 14. A XMCD signal of 16% is observed for 1 ML Mn/Fe and 13% for 2 ML. It should be noted that O’Brien and Tonner observed a similar effect for 1 ML Mn/Co,<sup>13</sup> which means that the Mn magnetic moment value is probably similar in each system. However, this XMCD signal is two times smaller than the one calculated by Wu and Freeman.<sup>16</sup> We have concluded that the *average* Mn magnetic moment is around  $1.7 \mu_B$ , as discussed in Ref. 14. Above 2 ML, the dichroic signal drastically changes (Fig. 9). Up to 4 ML, the films are still magnetic since a net dichroic signal is observed. Nevertheless, the shape of these dichroic signals is quite unusual and has never been observed on metallic films.

A possible explanation of the shape of the XMCD signal above 3 ML could be that the third Mn layer is ferromagnetic, its magnetic moment being antiparallel to the Mn moment of the underneath Mn layer. This assumption is supported by Walker and Hopster<sup>20</sup> who actually observed an antiferromagnetic stacking of Mn ferromagnetic planes above 3 ML. In this case, the dichroic signal could be interpreted as the superposition of two contributions with opposite sign if there is a chemical shift of around 0.5 eV between energy levels of both magnetic sites. Even if this value is not realistic in the case of metals, however, it is well known that the energy levels of an atom onto a flat surface are shifted compared to the ones of the same atom in the bulk. Such a “surface to bulk” energy shift between two AF coupled Mn moments could lead to such unusual XMCD signal.

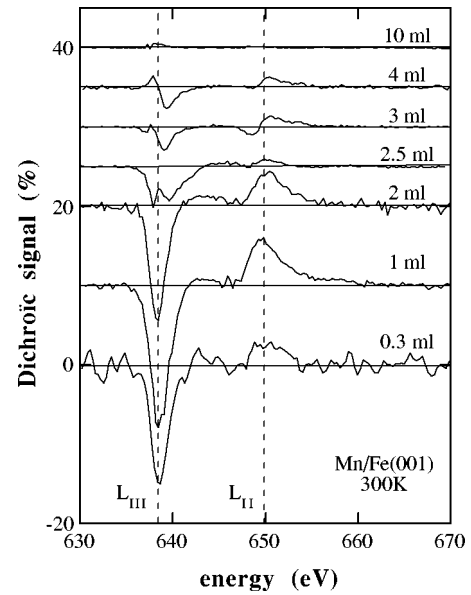


FIG. 9. XMCD spectra observed on Mn films from 0.3 to 10 ML thick. Note the drastic change of the XMCD shape above 2 ML.

For large thicknesses, the XMCD signal is almost zero, which means that the Mn films are nonmagnetic or antiferromagnetic. However, Walker and Hopster observed a Mn surface magnetic contribution<sup>20</sup> up to 20 ML thick, which means that these Mn films are in an AF state.

The structural and magnetic transition described above for free Mn thin layers on Fe(001) is no longer observed for Mn/Fe superlattices. In the latter case, the Mn structural transition is observed to occur for larger thicknesses. It is thus possible that Mn is in a ferromagnetic state in this bct structure up to 6 ML. In order to determine the corresponding Mn magnetic contribution, an XMCD experiment was performed on a 6 ML-thick Mn film capped with a 30 Å-thick Fe film. As shown in Fig. 10, no dichroic signal was observed. This 6

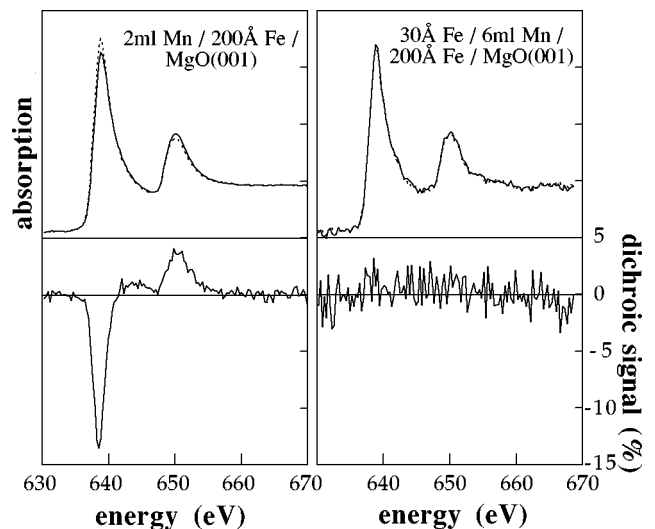


FIG. 10. Comparison between Mn  $L_{\text{II}}$ - $L_{\text{III}}$  edge and XMCD spectra measured on (left) a 2 ML-thick Mn film uncapped with Fe, and (right) a 6 ML-thick Mn film capped with a 30 Å-thick Fe film. In both samples Mn is in the bct structure described in the text.

ML-thick bct Mn film is thus antiferromagnetic. This analysis clearly demonstrates that the Mn ferromagnetic state observed on the uncapped Mn films in the 2 ML range is not stable for thicker Mn film prepared in the same structure.

#### IV. DISCUSSION AND CONCLUSION

In summary, uncapped Mn films are found to grow in a bct structure with  $a=2.87\pm 0.02$  Å and  $c=3.04\pm 0.04$  Å ( $c/a=1.06$ ) up to 2 ML on (001) bcc Fe lattice. This  $c$  value is lower than the value reported by Purcell *et al.*<sup>17</sup> However, Wu and Freeman<sup>25</sup> predicted a rather low  $c$  value for 2 Mn ML/(001) Fe and a qualitative experimental confirmation was recently given by Kim *et al.*<sup>24</sup> This low  $c$  value is definitely confirmed in this study. However, it should be noted that our results are not consistent with a  $c$  value lower than the (002) Fe value (1.43 Å), as proposed by these authors. At 3 ML, this bct structure is no longer stable. Indeed, a structural relaxation is observed, which can be explained by a relaxation of the surface stress as shown here by RHEED. Our results are consistent with an increase of the distance between Mn (001) planes. This is in agreement with the findings of Purcell *et al.*<sup>17</sup> and Kim *et al.*<sup>24</sup> These authors actually came to the conclusion that thick Mn films are bct with a  $c$  value close to 3.25 Å. However, we show in this study that this structural relaxation is undoubtedly more involved

since our results cannot be explained by assuming a fixed distance between Mn (001) planes.

Finally, we observe in uncapped Mn films that a magnetic transition from a ferromagnetic to an AF state comes with this structural transition. At this stage of the investigation, a conclusion that can be drawn is that this magnetic transition is due to this structural change. However, the analysis of structural and magnetic behaviors of Mn/Fe superlattices shows that this is not true. Indeed, in superlattices, this structural transition is observed to occur at larger thicknesses. The initial bct structure ( $c/a=1.06$ ) is actually found to be stable at least up to 6 ML at room temperature. However, the ferromagnetic behavior observed in the 0–2 ML uncapped Mn films is no longer stable for thick bct Mn films capped with Fe. These results demonstrate that the bct Mn structure is ferromagnetic on Fe when the Mn films are almost two dimensional, but not when the films are three dimensional. These results can be compared to recent theoretical investigations. Up to 1 ML, the Mn magnetic properties observed in this study can be explained by the occurrence of a ferrimagnetic state.<sup>16</sup> On the contrary, an antiferromagnetic state is predicted for bulk bct Mn.<sup>26</sup> This is again in agreement with our observations. The Mn ferromagnetic behavior observed in this study can thus only be attributed to the reduction of the Mn film dimension from three dimensions to two dimensions, as predicted theoretically.

\*Present address: European Synchrotron Radiation Facility (ESRF), BP 220, 38043 Grenoble Cedex, France.

<sup>1</sup>See, for instance, A. S. Arrott, and B. Heinrich, in *Metallic Multilayers and Epitaxy*, edited by M. Song, S. Wolf, and D. C. Gubser (The Metallurgical Society, 1988), p. 147.

<sup>2</sup>See M. T. Kief and W. Egelhoff, *Phys. Rev. B* **47**, 10 785 (1993), and reference therein.

<sup>3</sup>See, for instance, V. L. Moruzzi, *Phys. Rev. Lett.* **57**, 2211 (1986); P. M. Marcus and V. L. Moruzzi, *J. Appl. Phys.* **63**, 4045 (1988).

<sup>4</sup>F. Süss and U. Krev, *J. Magn. Magn. Mater.* **125**, 351 (1993).

<sup>5</sup>V. L. Moruzzi, P. M. Marcus, and J. Kübler, *Phys. Rev. B* **39**, 6957 (1989).

<sup>6</sup>B. Heinrich, A. S. Arrott, C. Liu, and S. T. Purcell, *J. Vac. Sci. Technol. A* **5**, 1935 (1987).

<sup>7</sup>Y. Nishihata, M. Nakayama, N. Sano, and H. Teraushi, *J. Appl. Phys.* **63**, 319 (1988).

<sup>8</sup>D. Tian, S. C. Wu, F. Jona, and P. M. Marcus, *Solid State Commun.* **70**, 199 (1989).

<sup>9</sup>W. F. Egelhoff, I. Jacob, J. M. Rudd, J. F. Cochan, and B. Heinrich, *J. Vac. Sci. Technol. A* **8**, 1582 (1990).

<sup>10</sup>K. Ounadjela, P. Vennègues, Y. Henry, A. Michel, V. Pierron-Bohnes, and J. Arabski, *Phys. Rev. B* **49**, 8561 (1994).

<sup>11</sup>S. Andrieu, H. Fischer, A. Traverse, and M. Piecuch, *Phys. Rev. B* **54**, 2822 (1996).

<sup>12</sup>V. L. Moruzzi and P. M. Marcus, *Phys. Rev. B* **38**, 1613 (1988).

<sup>13</sup>W. L. O'Brien, B. P. Tonner, G. R. Harp, and S. S. P. Parkin, *J. Appl. Phys.* **76**, 6462 (1994); W. L. O'Brien and B. P. Tonner, *Phys. Rev. B* **50**, 2963 (1994); **51**, 617 (1995).

<sup>14</sup>S. Andrieu, M. Finazzi, F. Yubero, H. Fischer, P. Arcade, F. Chevrier, L. Hennet, K. Hricovini, G. Krill, and M. Piecuch, *Europhys. Lett.* **38**, 459 (1997).

<sup>15</sup>S. Andrieu, M. Finazzi, F. Yubero, H. Fischer, P. Arcade, F. Chevrier, K. Hricovini, G. Krill, and M. Piecuch, *J. Magn. Magn. Mater.* **165**, 191 (1997).

<sup>16</sup>R. Q. Wu and A. J. Freeman, *Phys. Rev. B* **51**, 17 131 (1995); S. Mbirt, D. Erikson, B. Johanson, and H. L. Skriver, *ibid.* **52**, 15 070 (1995); O. Elmouhssine, P. Krüger, G. Moraitis, J. C. Parlebas, and C. Demangeat, *ibid.* **55**, R7410 (1997).

<sup>17</sup>S. T. Purcell, M. T. Johnson, N. W. E. McGee, R. Coehoorn, and W. Hoving, *Phys. Rev. B* **45**, 13 064 (1992).

<sup>18</sup>S. I. Zabinsky, J. J. Rehr, A. Andukinof, R. C. Albers, and M. J. Eller, *Phys. Rev. B* **52**, 2995 (1995).

<sup>19</sup>C. T. Chen, F. Sette, Y. Ma, and S. Modesti, *Phys. Rev. B* **42**, 7262 (1990).

<sup>20</sup>T. G. Walker and H. Hopster, *Phys. Rev. B* **48**, 3563 (1993).

<sup>21</sup>S. Andrieu, F. Arnaud d'Avitaya, and J. C. Pfister, *J. Appl. Phys.* **65**, 2681 (1989).

<sup>22</sup>J. Massies and N. Grandjean, *Phys. Rev. Lett.* **71**, 1411 (1993); J. Fassbender, U. May, B. Schirmer, R. M. Jungblut, B. Hillenbrands, and G. Guntherodt, *ibid.* **75**, 4476 (1995).

<sup>23</sup>J. Dresselhaus, D. Spanke, F. U. Hillebrecht, E. Kisker, G. Van der Laan, J. Goedkoop, and N. B. Brookes, *Surf. Sci.* **377-379**, 450 (1997).

<sup>24</sup>S. K. Kim, Y. Tian, M. Montesano, F. Jona, and P. M. Marcus, *Phys. Rev. B* **54**, 5081 (1996).

<sup>25</sup>R. Wu and A. J. Freeman, *J. Magn. Magn. Mater.* **161**, 89 (1996).

<sup>26</sup>P. Krüger, O. Elmouhssine, C. Demangeat, and J. C. Parlebas, *Phys. Rev. B* **54**, 6393 (1996).